XENOCRYST ORIGIN OF PYROXENE AND PLAGIOCLASE IN ENRICHED HIGH-TI BASALT CLAST FROM LUNAR METEORITE DHOFAR 1428.

Zhuqing Xue[1], Long Xiao[1,*], and Clive R. Neal[2], [1]Planetary Science Institute, China University of Geosciences, Wuhan, China (2533149235@qq.com), [2]Department of Civil Engineering and Geological Sciences, University of Notre Dame, Notre Dame, Indiana 46556, U.S.A..

Introduction: Basaltic lunar meteorites are good candidates to understand many controversies about the composition and evolution of the Moon, and the petrogenesis of different kinds of basalts. But so far, little attention has been paid to the basalt clasts in feldspathic breccias that have the potential to expand our knowledge to resolve these controversies. We describe an enriched high-Ti basalt clast in lunar meteorite NWA 1428, an incompatible trace element-poor feldspathic breccia, and then present detailed petrological and geochemical survey of this basalt clast to add data to understanding the origin and evolution of enriched mare basalts.

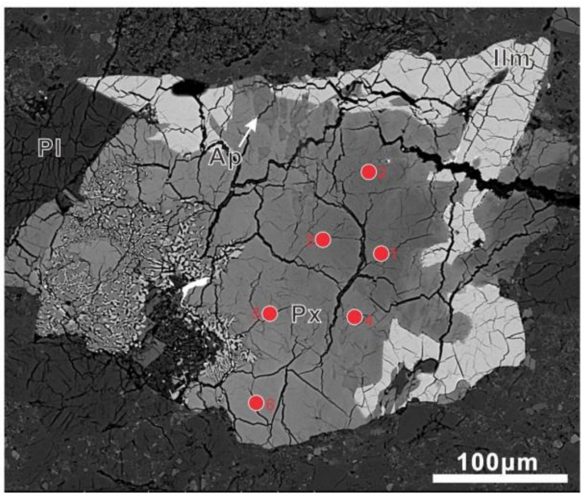

Figure 1 Back scatter electron (BSE) image of the enriched high-Ti basalt in Dhofar 1428, the six red circles show LA-ICP-MS spots.

Analytical Methods: The basalt clast petrography was examined by scanning electron microscopy (FE-SEM, FEI Quanta 200). Major element mineral data were determined using electron probe micro-analysis (EPMA; JEOL JXA8230). In situ trace element mineral data were determined on pyroxene and plagioclase using laser ablation inductively coupled plasma mass spectrometer (LA-ICP-MS). All of these analysis were conducted at the State Key Laboratory of Geological Processes and Mineral Resources, China University of Geosciences, Wuhan, China.

Whole rock major and trace element compositions of the basalt clast, including the whole rock minus Mg-pyroxene and plagioclase were estimated according to mineral compositions and their area proportions. Trace element partition coefficients for clinopyroxene and plagioclase are calculated using the relevant EPMA data using the method in [1,2] at T=1200°C.

Resultss:

Petrography and major element compositions. The basalt consists of relatively large, zoned pyroxenes, elongated ilmenite and plagioclase laths, plus late-stage phases such as symplektites, Si-K-Al assemblages, apatites, K-feldspar, and a baddeleyite lath (Figure 1). The symplektites are myrmekitic intergrowths of hedenbergite + fayalite + silica.

Plagioclases are relatively Ab-rich ($An_{72-72.6}$), and pyroxenes exhibit complex Fe-Mg-Ca zonations ($En_{12.2-47}Fs_{17.7-72.2}Wo_{15.3-36.6}$, $Mg^{\#}$=14.5-72.6), which are consistent with pyroxenes reported in Apollo high-Ti basalts [3] in the diagram of $Ti^{\#}$-$Fe^{\#}$ (Figure 2).

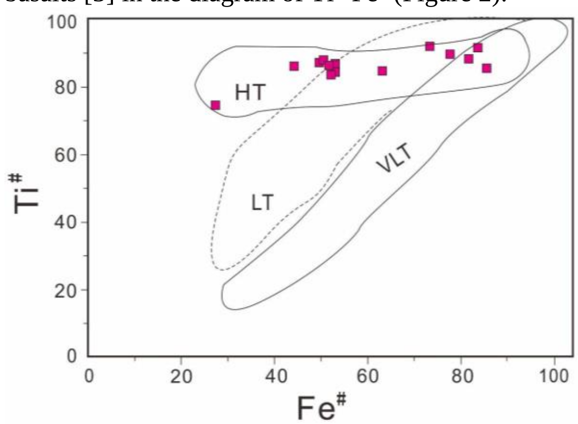

Figure 2 Plot of Ti vs. Fe for pyroxenes from the enriched high-Ti basalt clast.

Trace element compositions. Plagioclase is LREE-rich and with positive Eu anomalie (Figure 3a). However, REE patterns of pyroxenes are more complex, they all show deep negative Eu anomalies and can be divided into two groups: the relative magnesian cores (PX1-4, $Mg^{\#}$ = 47.43-50.34) have relative flat REE patterns (La/Lu_N = 0.26-0.69, Figure 3a), while the ferrous rims (PX5-6, $Mg^{\#}$=16.41-19.45) are HREE-rich (La/Lu_N = 0.08, Figure 3a).

Like the REE patterns of pyroxene zonations, the calculated equilibrium liquids of them are also dichotomous: with those of Mg-pyroxenes displaying enriched LREE and flat to enriched HREE patterns (Figure 3b), while those of Fe-pyroxenes are depleted in LREE (Figure 3b). Similar to equilibrium liquids of Mg-pyroxenes, the calculated equilibrium liquid of plagioclase is also LREE-rich and show flat to enriched

HREE character (Figure 3b). In addition, equilibrium liquids of plagioclase and Mg-pyroxenes are not sub-parallel to that of the calculated whole rock, but those of Fe-pyroxenes are (Figure 3b).

Discussion: The fact that equilibrium liquid REE patterns of plagioclase and Mg-pyroxene are not sub-parallel to that of the calculated whole rock, but those of Fe-pyroxenes are, indicates the Mg-pyroxenes and plagioclases may not be in equilibrium and could be xenocrysts. Furthermore, the REE profile of the Mg-pyroxenes and plagioclase-subtracted whole rock is also presented in Figure 3b, which is LREE depleted and subparallel to the equilibrium liquids from the Fe-pyroxenes.

Conclusion: The calculated equilibrium liquids are interpreted to show that the Mg-pyroxenes and plagioclases are xenocrysts that were entrained by an unrelated magma. Fe-pyroxene crystallized as overgrowths on the Mg-pyroxene xenocrysts. In addition, equilibrium liquids of these xenocrysts are HREE-enriched compared with typical KREEP basalts 15386 [4], average Apollo 17 KREEP basalt [5], and high-K KREEP [6] (Figure 3b). This indicates that enriched liquids existed within lunar interior that had different REE patterns and elevated REE relative to typical KREEP basalts in the existing sample collection.

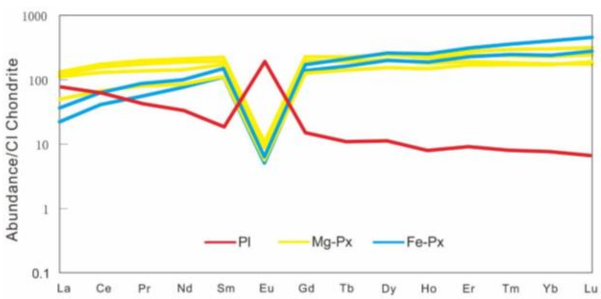

Figure 3a REE patterns of pyroxenes and plagioclase within the enriched high-Ti basalt.

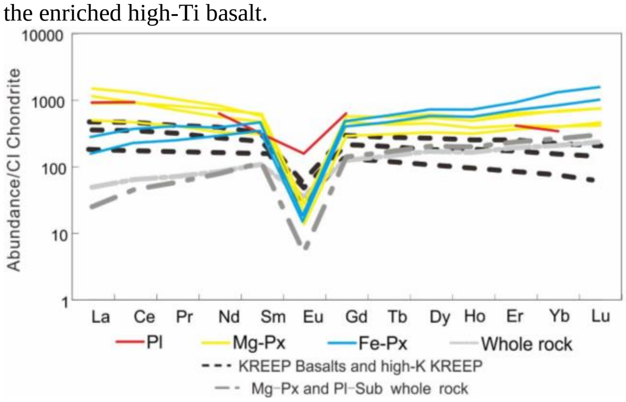

Figure 3b REE patterns of equilibrium melts of pyroxenes and plagioclase compared with KREEP basalts [4,5], high-K KREEP [6], and whole rock including Pl+Mg-Px-Sub whole rock.

This work demonstrated that trace element analyses of minerals, especially zoned minerals, can uncover details of magma evolution in small breccia clasts that add to our knowledge of lunar magmatic systems and pathways.

Acknowledgments: This study was supported by granted by Natural Science Fundation of China (41772050) and the research grant of State Key Laboratory of Isotope Geochemistry, Guangzhou Institute of Geochemistry, Chinese Academy of Sciences (SKLab-IG-KF-16-14).

References: [1] Sun C. and Liang Y. (2012) *Contrib. Mineral. Petrol.*, 163, 807-823. [2] Hui H. et al. (2011) *Geochim. Cosmochim. Acta,* 75, 6439-6460. [3] Robinson K. and Treiman A. (2010) *LPS XXXXI*, Abstract 1788. [4] Neal C. and Kramer G. (2003) *LPS XXXIV*, Abstract 2023. [5] Salpas P.A. et al. (1987) *JGR*, 92, 340-348. [6] Warren P.H. (1989) *LPI Tech. Rpt*, 89, 149-153.